

Étude structurale de matériaux sous forme de couches minces par diffraction des rayons X en incidence rasante

G. Baldinozzi, D. Simeone

SPMS, LRC Carmen, CNRS-CEA-CentraleSupélec

J-F Bérar

Néel, Grenoble

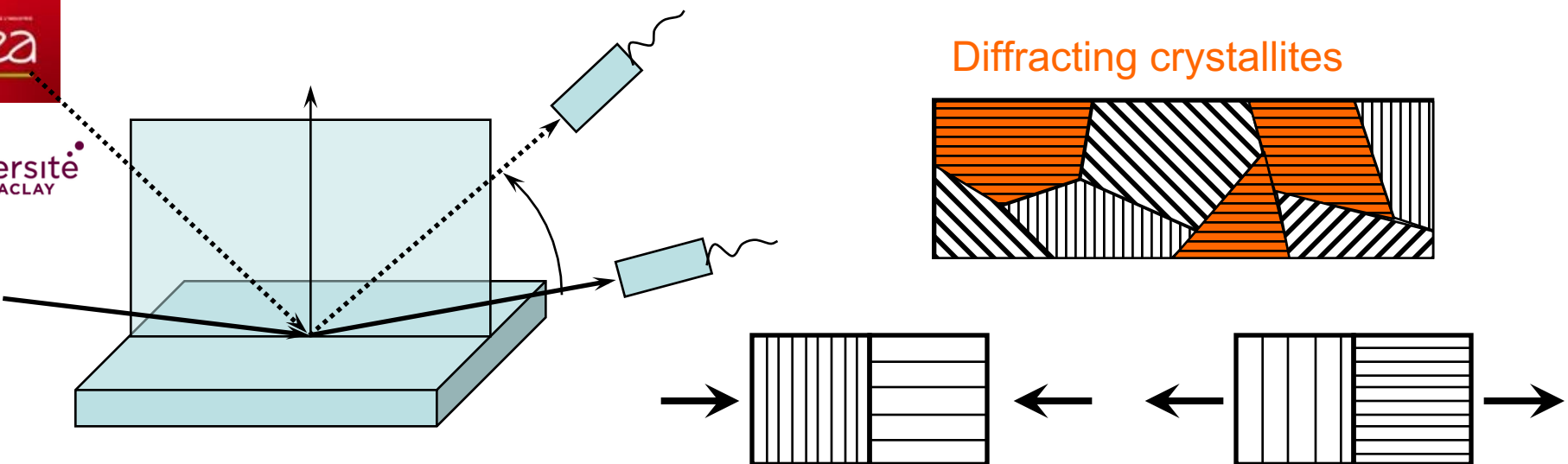
Collaborations et exemples d'applications:

- S. Bouffard (Cimap, Caen), P. Lecoeur (IEF, Orsay)
C. Laberty-Robert, C. Sanchez (LCMC, Jussieu)

*ANR-06-BLAN-0292, C'nano IDF Solnac 2009,
Triangle de la Physique Instrumat 2011-074T, ANR-10-LABX-0039*

Outline

- Diffraction basics – Glancing angle (incidence) XRD**
- Rietveld method and GA-XRD**
- Structures & microstructures**
- Examples**
- Conclusion**



- + Reliable information on
 - the preferred orientation of crystallites
 - the crystallite size and lattice strain (in one direction)
- No information on the residual stress (constant direction of the diffraction vector)
- Low scattering from the layer (large penetration depth)

L.G. Parratt, Surface Studies of Solids by Total Reflection of X-rays, Physical Review 95 (1954) 359-369.

université PARIS-SACLAY

$$n = \sqrt{1 + \chi} \approx 1 + \frac{\chi}{2} = 1 - \frac{r_e \lambda^2}{2\pi} \rho$$

$$n \approx 1 - \frac{r_e \lambda^2}{2\pi} \rho_e (f_0 + f' - if'')$$

$$n \approx 1 - \delta + i\beta \leq 1$$

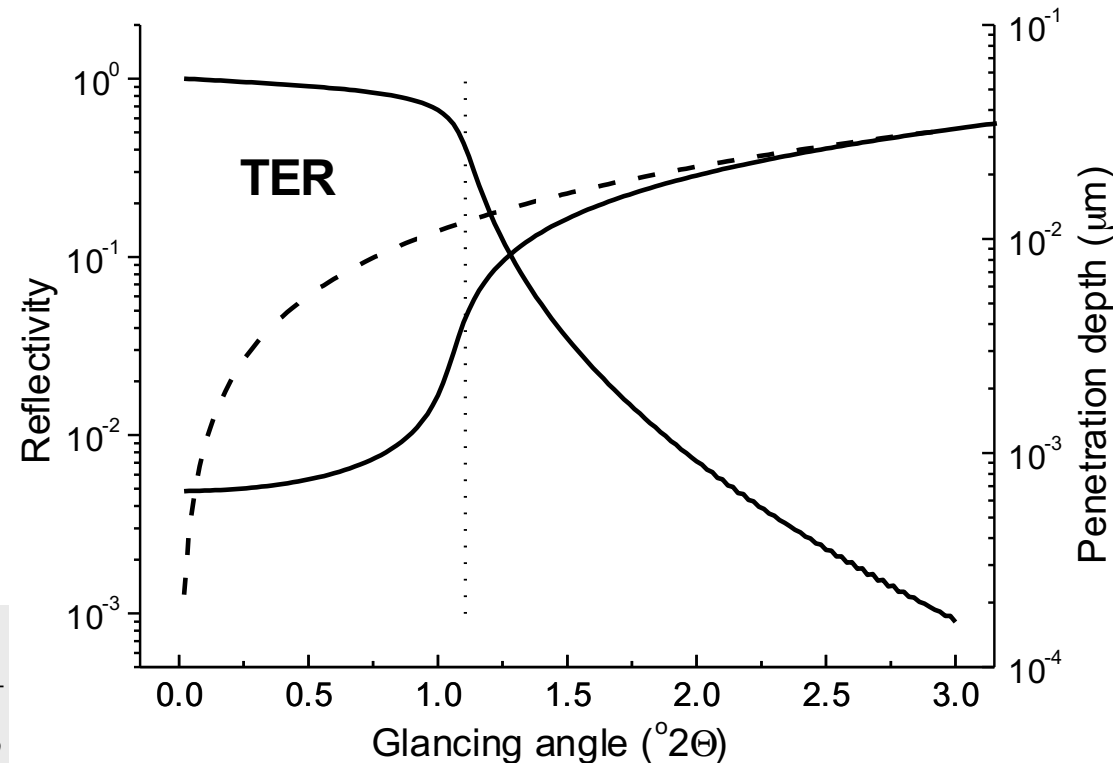
Example: Gold (CuK α)

$$\delta = 4.2558 \times 10^{-5}$$

$$\beta = 4.5875 \times 10^{-6}$$

$$n_V \cos \theta = n_j \cos \theta_j \quad ; \quad n_j = \cos \theta_c$$

$$1 - \frac{r_e \lambda^2}{2\pi} \rho \cong 1 - \frac{\theta_c^2}{2} \quad ; \quad \theta_c \cong \sqrt{\frac{r_e \lambda^2}{\pi}} \rho$$



Snell, Fresnel laws for X-rays (GAXRD)

$$\psi_j = a_j e^{i \vec{k}_j \cdot \vec{r}} ; j=I, T \text{ or } R \quad k = |\vec{k}_I| = |\vec{k}_R| = \frac{1}{n} |\vec{k}_T|$$

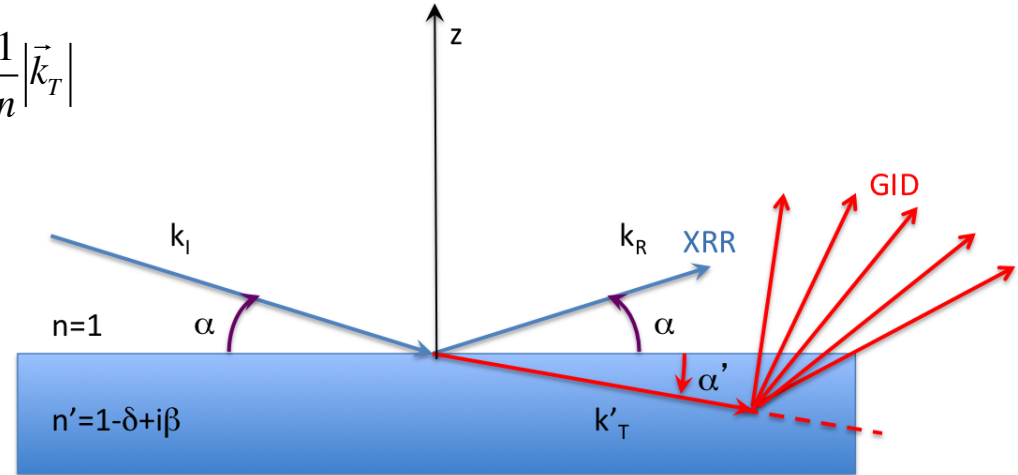
$$C^1 \quad \begin{cases} a_T = a_I + a_R \\ a_T k_T = a_I k_I + a_R k_R \end{cases}$$

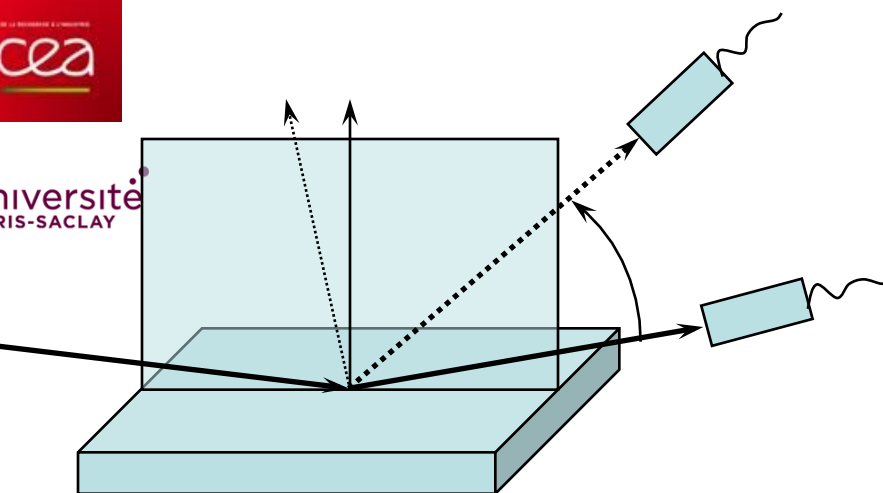
$$\begin{cases} n \cos \alpha' = \cos \alpha \\ (a_I + a_R) n \sin \alpha' = (a_I - a_R) \sin \alpha \end{cases}$$

$$n = 1 - \delta + i\beta \equiv 1 - \frac{\alpha_c^2}{2} + i\beta ; \alpha_c^2 \equiv \left(\frac{4\pi}{k^2} \right) \rho , \beta = \frac{\mu}{2k}$$

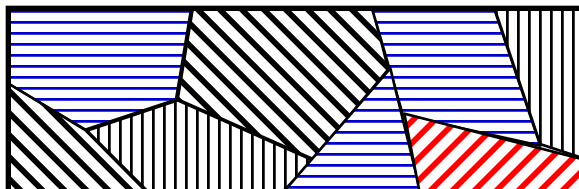
$$\left(1 - \frac{\alpha_c^2}{2} + i\beta \right) \left(1 - \frac{\alpha'^2}{2} \right) = \left(1 - \frac{\alpha^2}{2} \right) \rightarrow \alpha'^2 = \alpha^2 - \alpha_c^2 + 2i\beta \quad \text{Snell's Law}$$

$$\left(1 + \frac{a_R}{a_I} \right) \alpha' = \left(1 - \frac{a_R}{a_I} \right) \alpha \rightarrow R \equiv \frac{a_R}{a_I} = \frac{\alpha - \alpha'}{\alpha + \alpha'} \quad \text{Fresnel's Law}$$

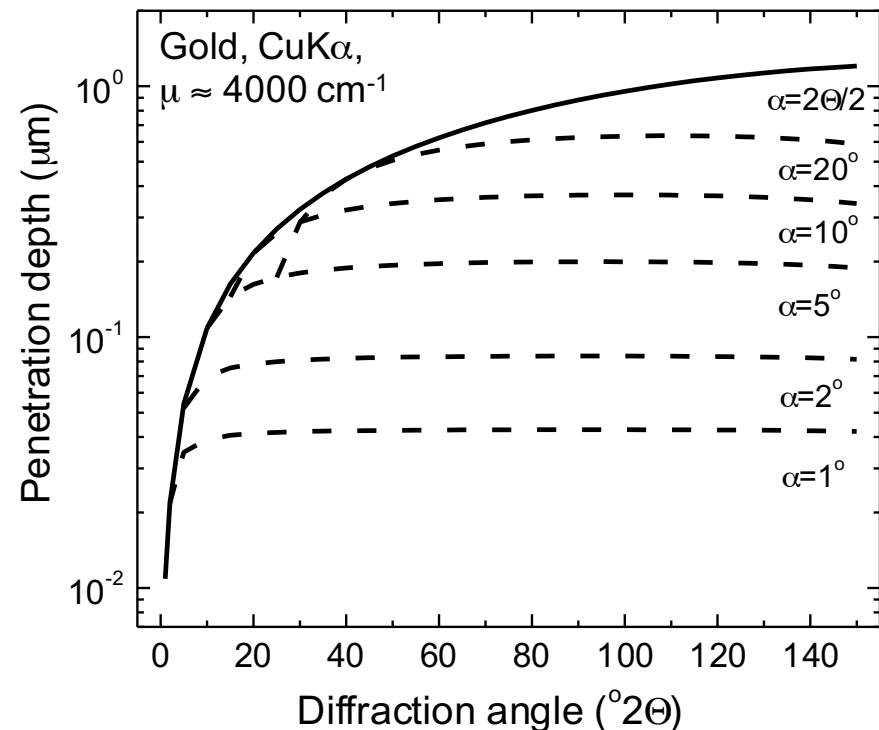




GAXRD



$$t : \frac{dI}{dz} = I_0 \frac{1}{e}; x_e = \frac{\sin \theta_i \cdot \sin \theta_o}{\mu(\sin \theta_i + \sin \theta_o)}$$

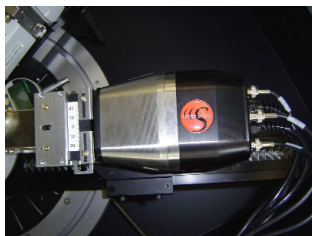
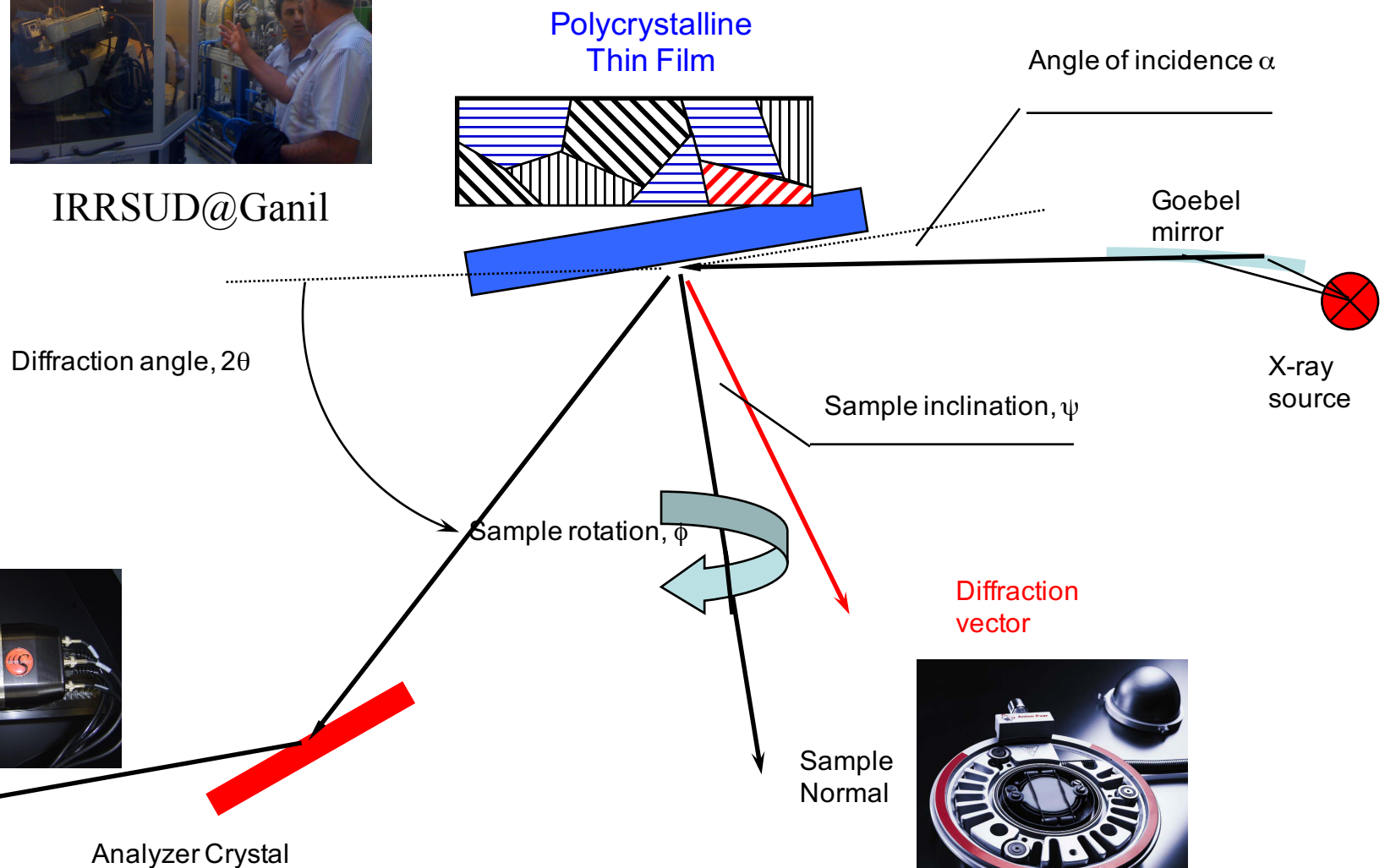


GAXRD Basics

- Parallel, monochromatic X-ray beam impinges on a sample surface at a fixed angle of incidence (α_I) and diffraction profile is recorded by detector-only scan.
- When the angle of incidence (α_I) of X-ray beam decreases, since the refractive index in the sample is less than unity, total external reflection of X-rays occurs below the critical angle of incidence α_C . The diffracted and scattered signals at the angle 2θ arise mainly from a limited depth below the surface of the specimen.

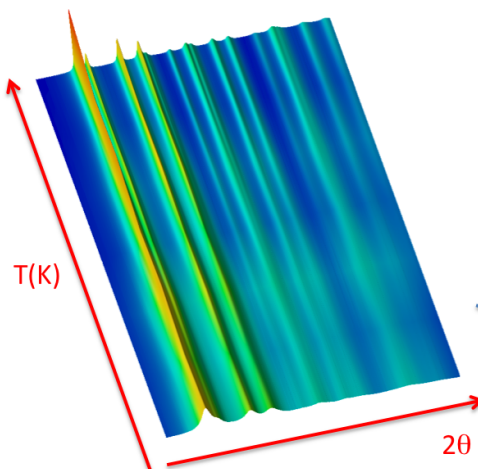


IRRSUD@Ganil

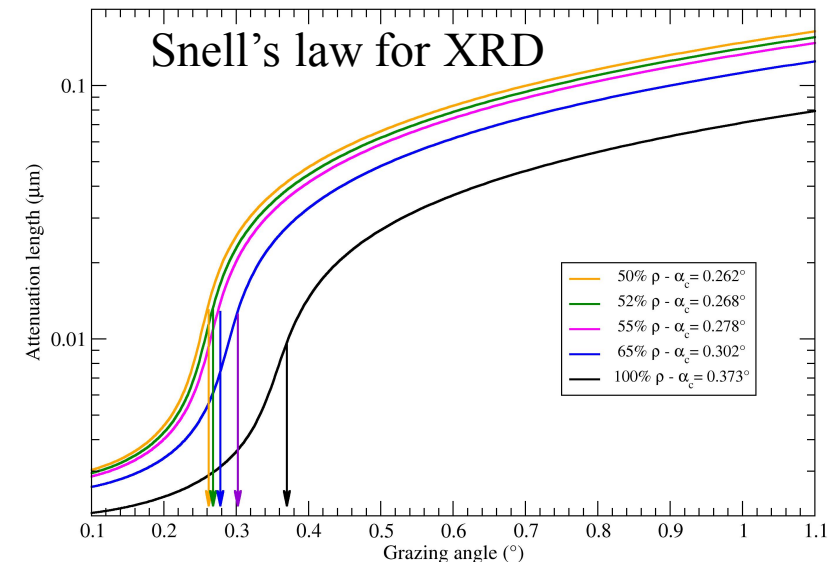
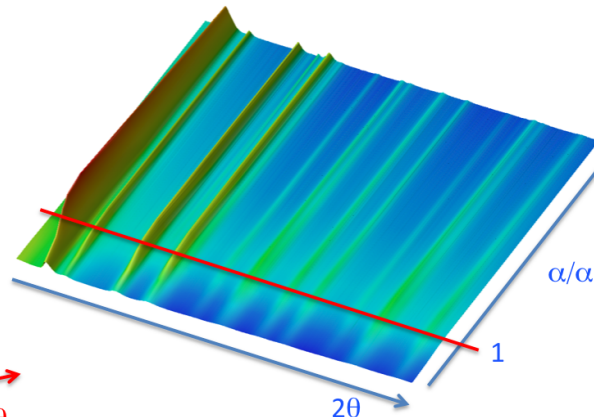


- Quantitative phase analysis
- Symmetry
- Crystal structure (Rietveld)
- Crystallite size and strain determination

Isothermal annealing



Microstructure vs. depth



$$1 + R(\alpha) = T(\alpha) \rightarrow T(\alpha) = \frac{2\alpha}{\alpha + \alpha'}$$

$$T(\alpha) = \frac{2\alpha/\alpha_c}{\alpha/\alpha_c + \sqrt{(\alpha^2/\alpha_c^2 - 1)}} \text{ for } \alpha > \alpha_c$$

$$T(\alpha) = 2 \frac{\alpha}{\alpha_c} \text{ for } \alpha \leq \alpha_c$$

Reflections shape and breadth ...

- Instrumental broadening**
- Specimen-related broadening**
 - Crystallite finite size
 - Microstrain
 - ✓ Non-uniform Lattice Distortions
 - ✓ Faults
 - ✓ Dislocations
 - ✓ Antiphase domain boundaries
 - ✓ Surface Relaxation
 - ✓ ...
- The peak profile is a convolution of the effects from all of these contributions**

Typical sources of instrumental broadening

□ X-ray Source Profile

- Natural emission linewidths of $K\alpha_1$ and $K\alpha_2$ lines
- Size of the X-ray source

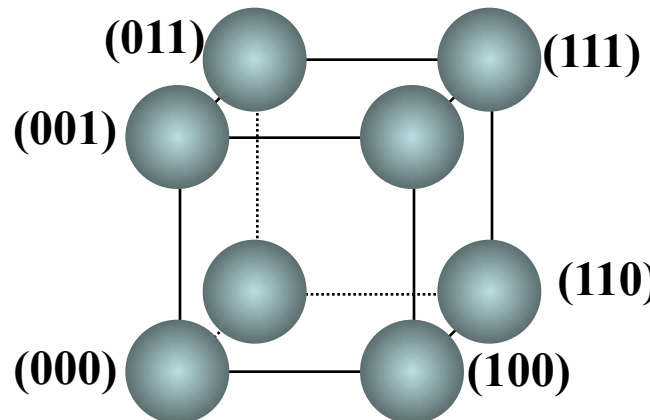
□ Goniometer Optics

- Divergence and Receiving Slit widths
- Imperfect focusing
- Beam size
- Penetration into the sample
- ...

Specimen broadening

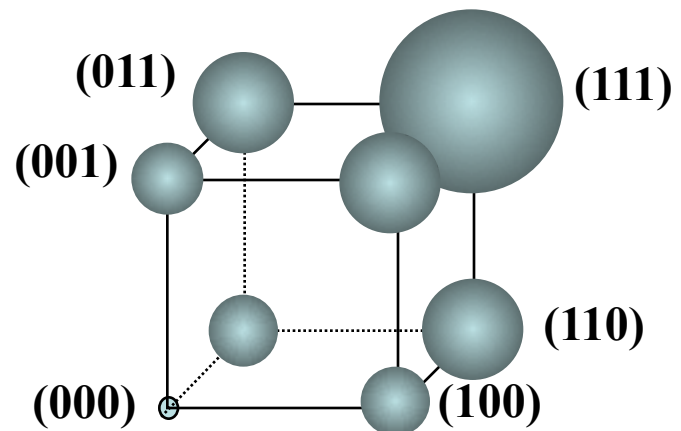
Crystallite size

- Fourier transformation of finite objects (with limited size)
- Constant line broadening (with increasing diffraction vector)



Lattice strain

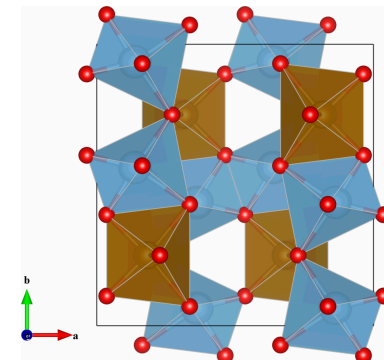
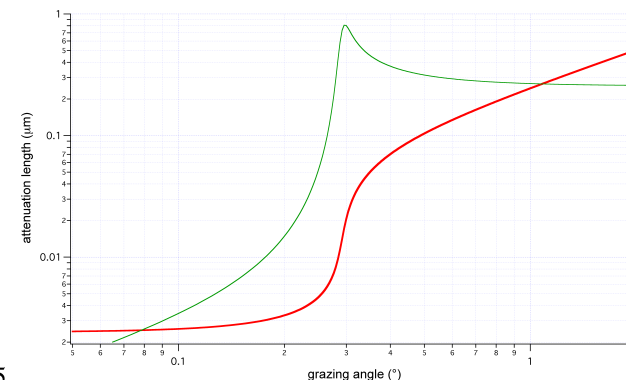
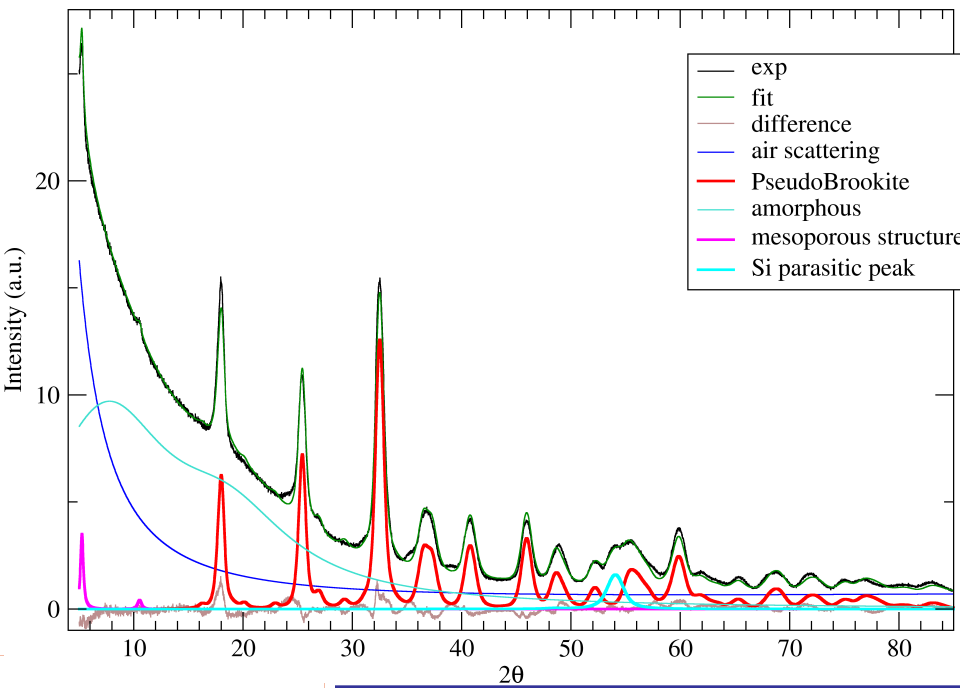
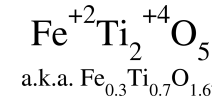
- Local changes in the d-spacing
- Line broadening increases with increasing q (a result of the Bragg equation in the differential form)



Rietveld and GAXRD: XND software

- Empirical profile matching is sometimes difficult:
 - overlapping peaks
 - a mixture of nanocrystalline phases
 - a mixture of nanocrystalline and microcrystalline phases
- Rietveld profile analysis (more information about the sample)
 - how much of each phase is present in a mixture
 - lattice parameter refinement
 - ❖ nanophase materials often have different lattice parameters from their bulk counterparts
 - atomic structure, site occupancy, thermal displacement parameters, ...
 - better compensation of profile-related errors

Rietveld analysis of multi-phase thin films



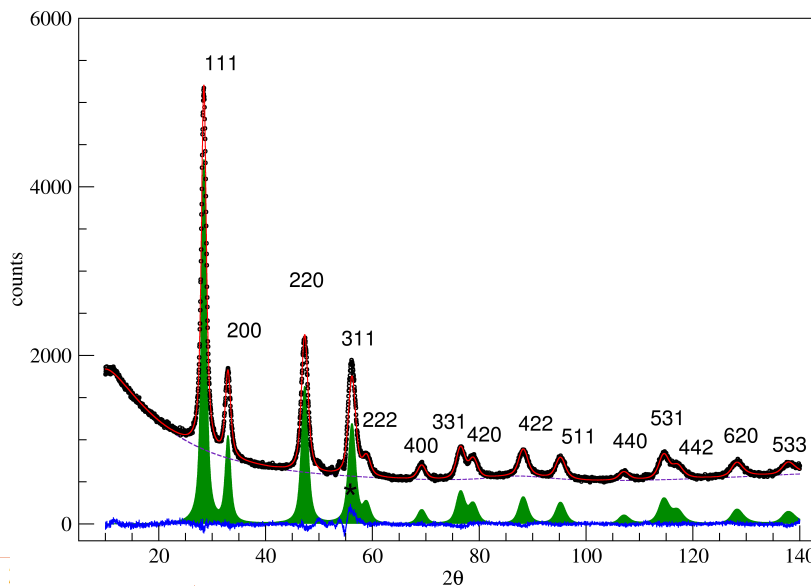
- Accurate retrieval of “domain” size and microstrain once instrumental broadening is corrected for
- Increased sensitivity to layers immediately below the surface
- In-situ measurements (irradiation and/or annealing phases)

J. Mat. Chem A 2 6567-6577 (2014)

Measuring structure and strain in a thin layer: thin films & the problem of ion irradiation

□ The GAXRD setup

- Accurate retrieval of “domain” size and microstrain once instrumental broadening is corrected for
- Increased sensitivity to layers immediately below the surface
- In-situ measurements (irradiation and/or annealing phases)



Typical GAXRD pattern
obtained on a fluorite phase

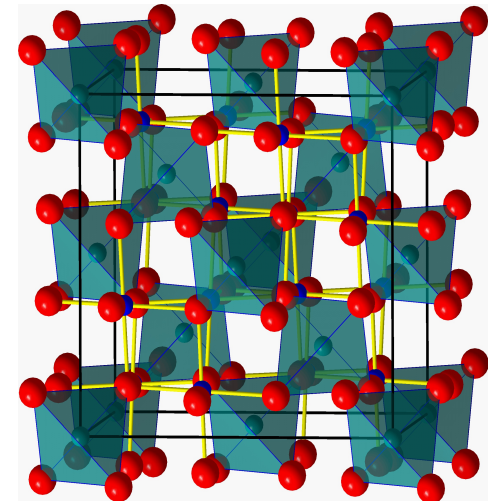
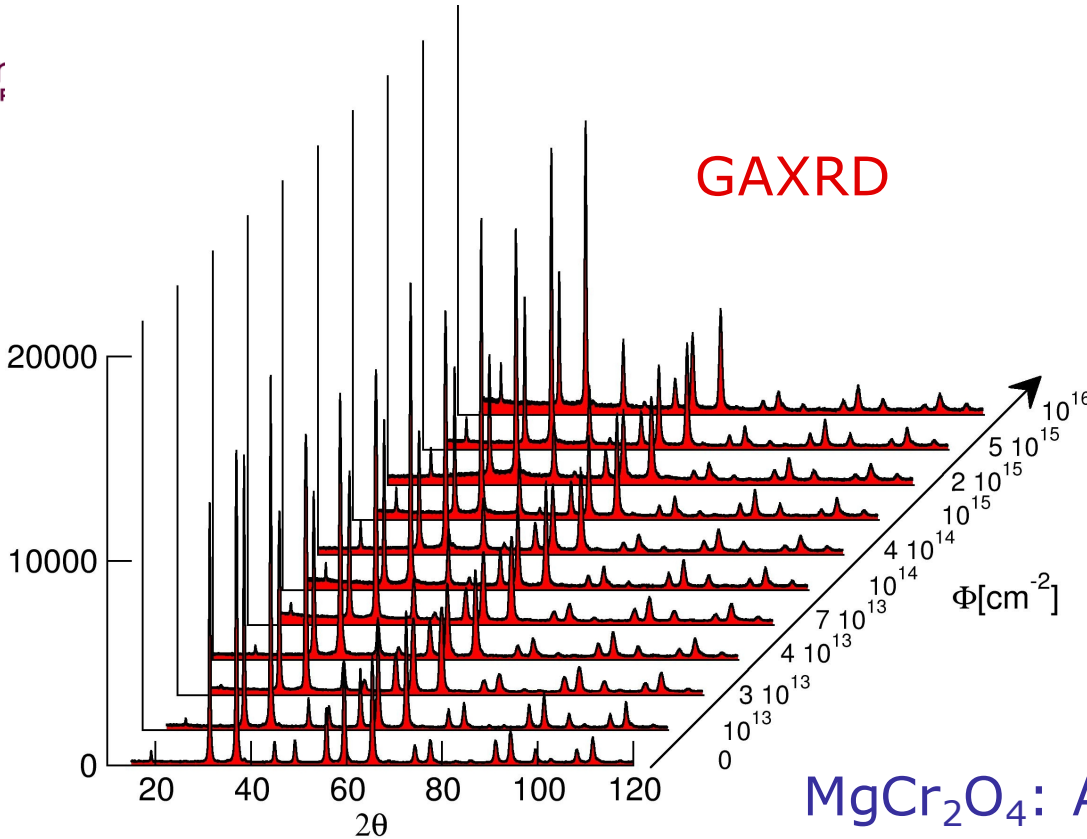
Structural evolution of spinels under irradiation

Behavior of spinel under irradiation: Modification of Diffraction patterns

	MgAl_2O_4	MgCr_2O_4	ZnAl_2O_4
High E. ions @RT	Vanishing of odd Bragg reflexions D. Simeone, J. Nucl. Mat. 2002 K Yasuda, MINB 2006, JNM 2007...	Vanishing of odd Bragg reflexions G. Baldinozzi, Nucl. Inst Meth B. 2007	Non vanishing of odd Bragg reflexions D. Simeone, J. Nucl. Mat. 2002
Low E. ions @ 140 K	Vanishing of odd Bragg reflexions L.M. Wang, MRS 1995, R. Devanathan, Phil Mag Let 1995		
Low E. ions @ RT	Non vanishing of odd Bragg reflexions D. Gosset, J. Eur. Ceram. 2005	Vanishing of odd Bragg reflexions D. Gosset, J. Eur Ceram Soc, 2005	Non vanishing of odd Bragg reflexions G. Baldinozzi, Nucl. Inst Meth B. 2005

Spinel irradiation at room temperature

Simulation of neutron irradiation by low energy ions (cascades) and of fission products by swift heavy ions



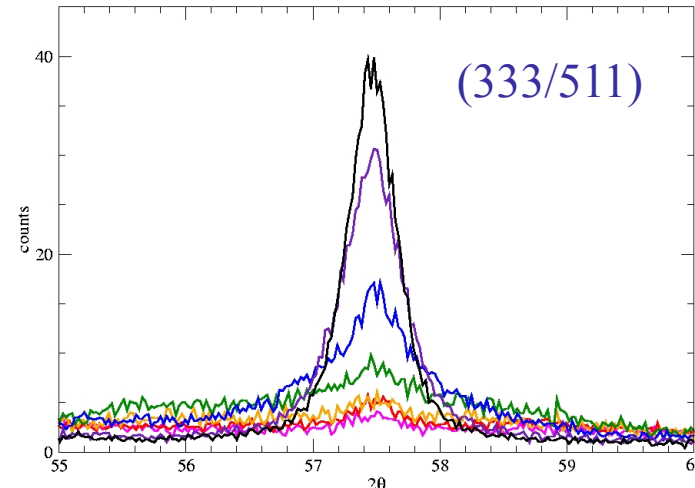
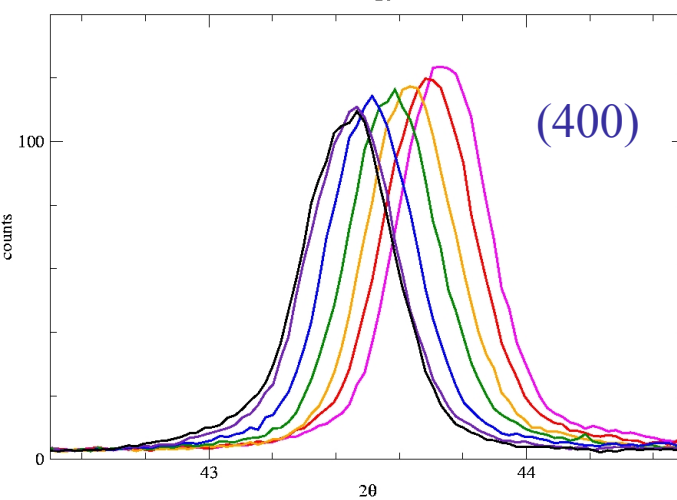
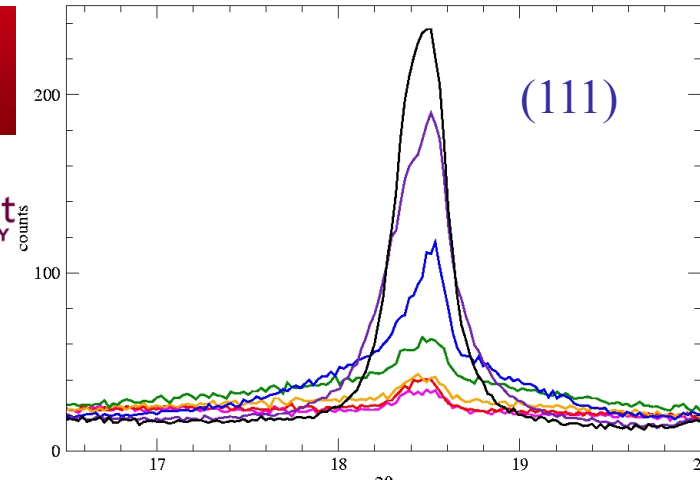
GAX-Ray diffraction:
Asymmetric reflection setup (fixed,
grazing impinging beam)

MgCr_2O_4 : Au @ 4 MeV

MgCr₂O₄: thermal annealing after irradiation

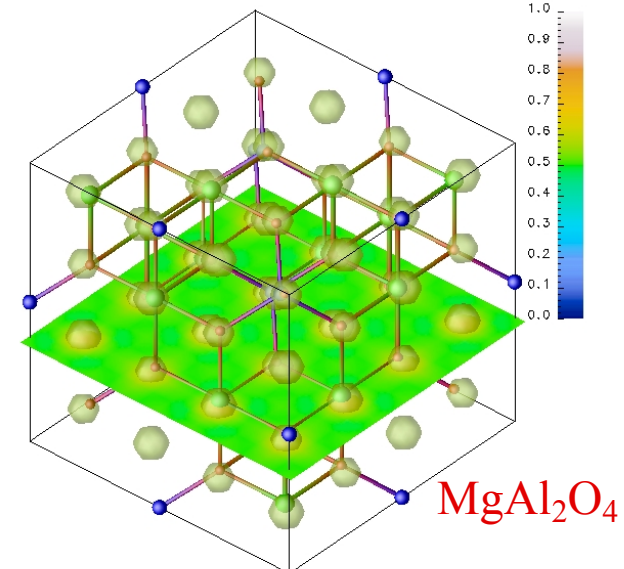
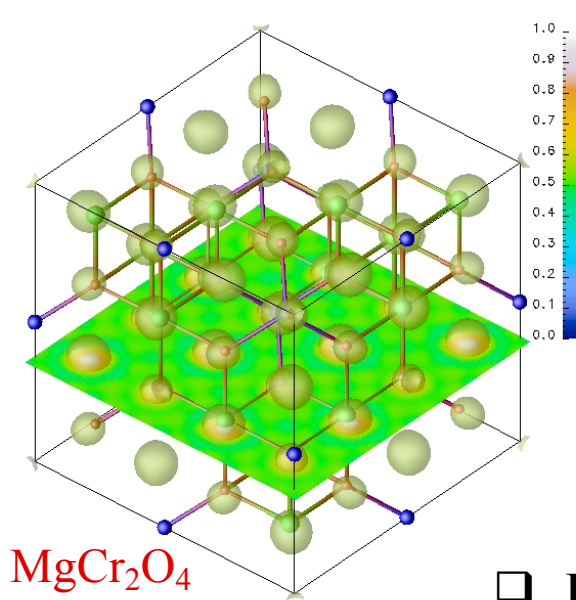
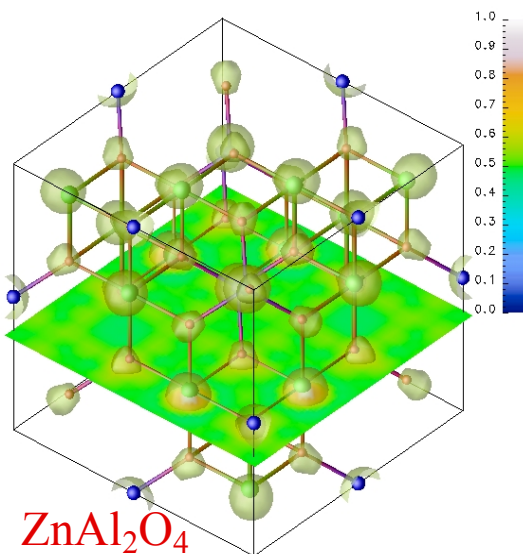


université
PARIS-SACLAY

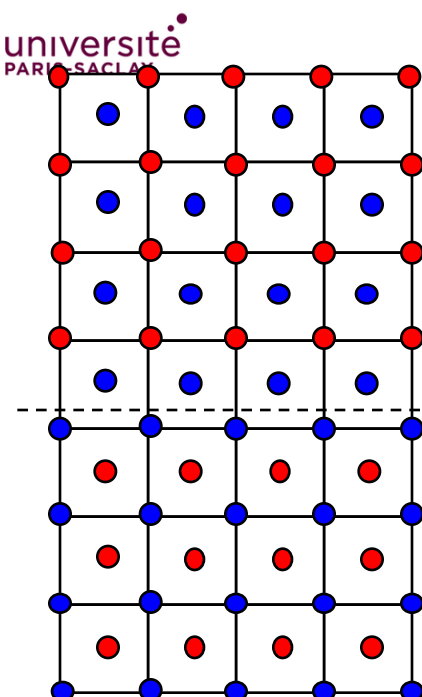


- Temperature restores the normal structure.
- The annealing of the extended defects increases the size of the coherent diffracting domains.

Electron density from X-ray diffraction



- Fourier syntheses derived from the observed diffracted intensities indexed in the $\text{Fd}3\text{m}$ space group



How to reconcile LRO & SRO?

- Ion irradiation produces changes in the structures of spinels:

- At the atomic scale:

- ✓ Cations are interchanged as in the thermal picture
 - ✓ The local structure consists of octahedra and tetrahedra
 - ✓ The “true” space group is unchanged

- The existence of extended defects produces

- ✓ A broadening of (ooo) peaks
 - ✓ An apparent symmetry change to the Fm3m ($a' = a/2$)

- Antiphase domain boundaries?

- Formed during the ordering of a material that goes through an order-disorder transformation
 - The fundamental peaks are not affected
 - The superstructure peaks are broadened
 - ✓ the broadening of superstructure peaks varies with hkl

Mesoporous ceria layers (coarsening)

μ -SOFC

Cermet: Ni/Ce_{0.9}Gd_{0.1}O_{2-x} porous

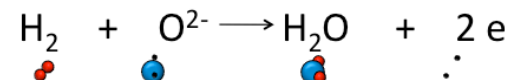
Fuel
Anode

≈ 200 nm

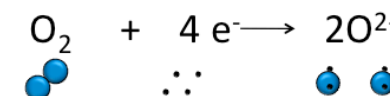
Electrolyte
 ≈ 600 nm

Cathode
 ≈ 200 nm

Air

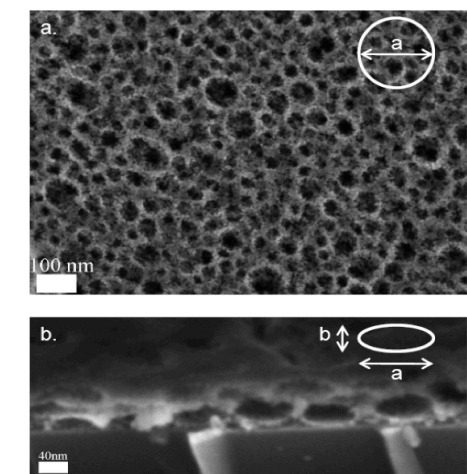
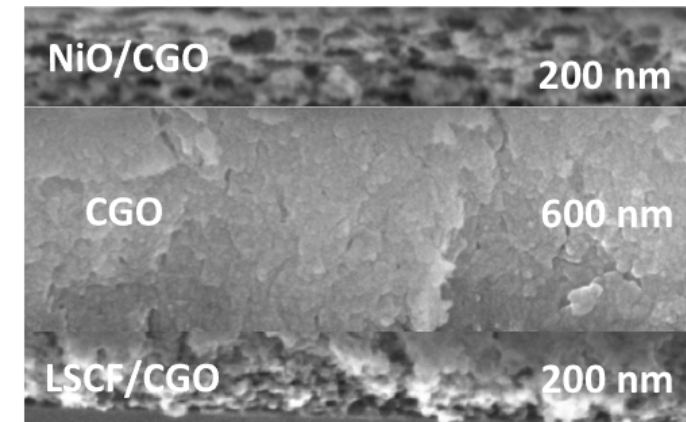


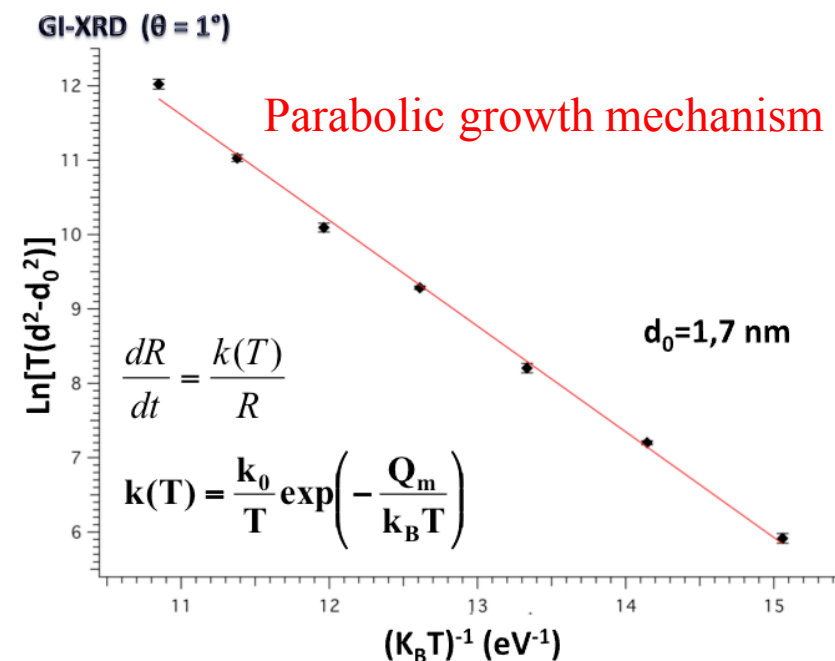
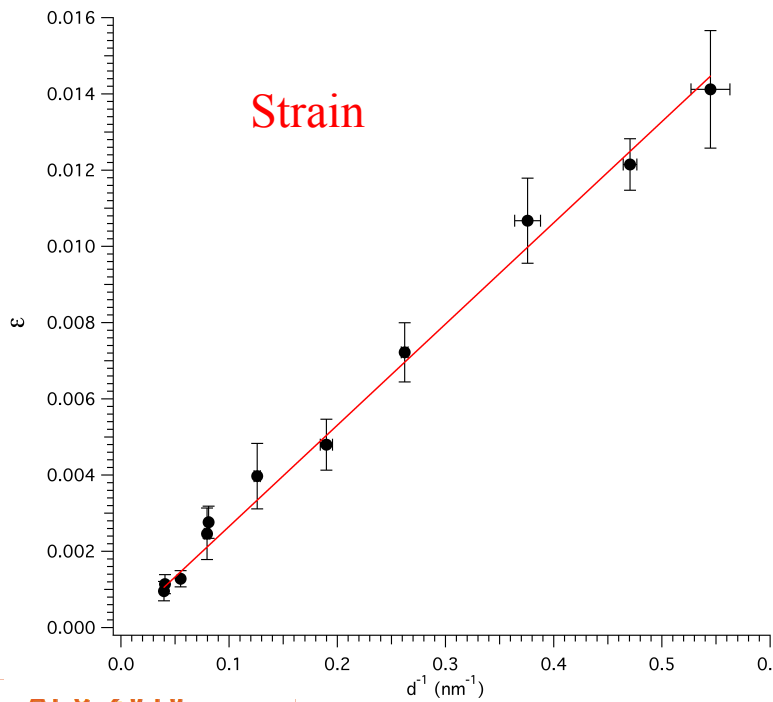
Ceramic: Ce_{0.9}Gd_{0.1}O_{2-x} dense



Total Thickness
 $\leq 1 \mu\text{m}$

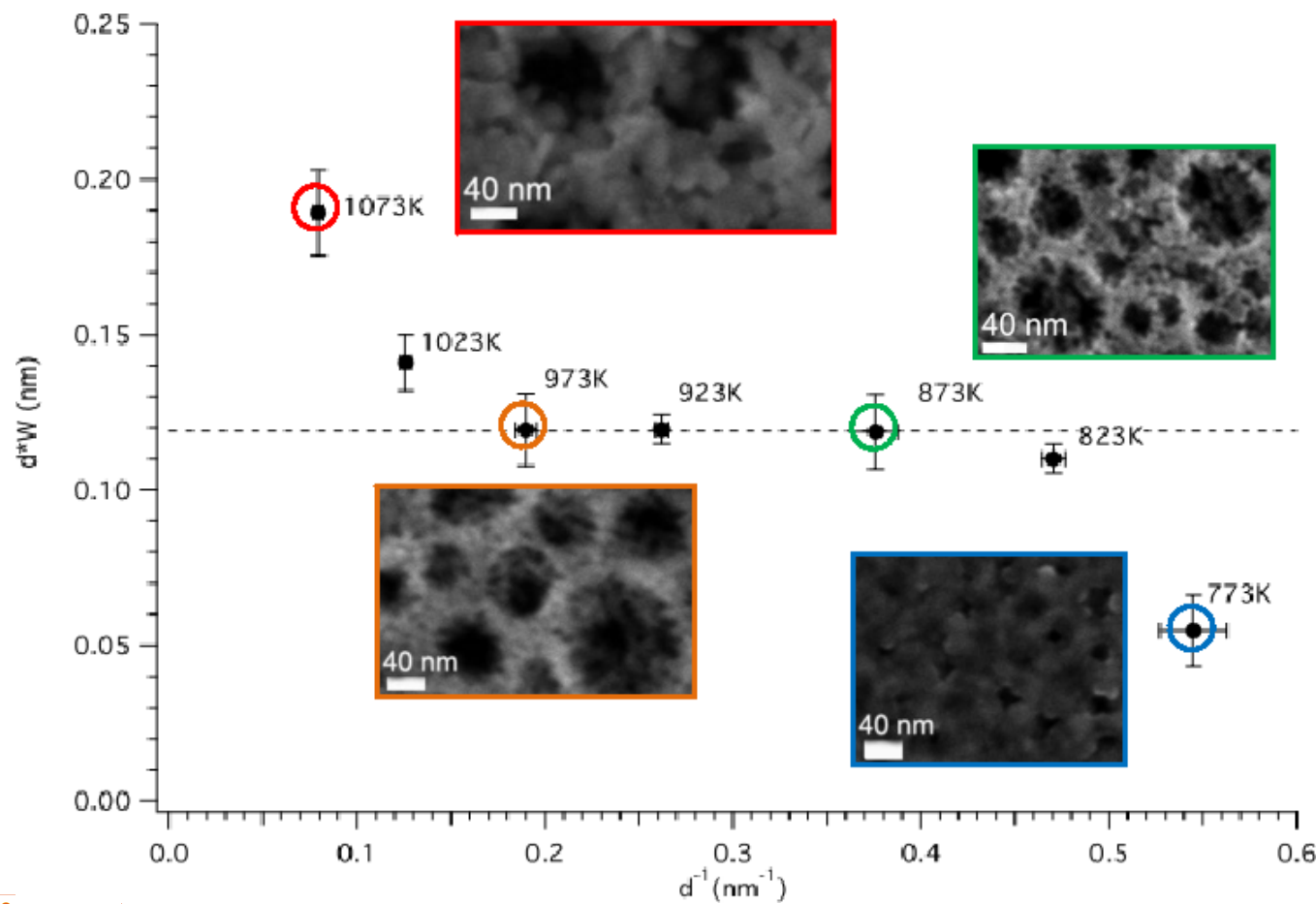
Composite: LSCF/Ce_{0.9}Gd_{0.1}O_{2-x} porous



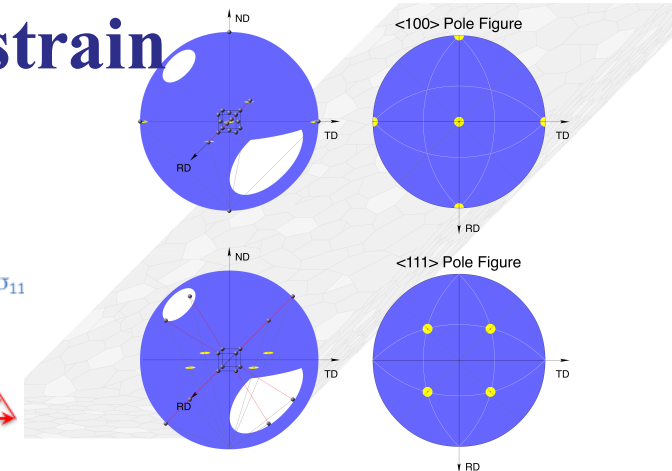
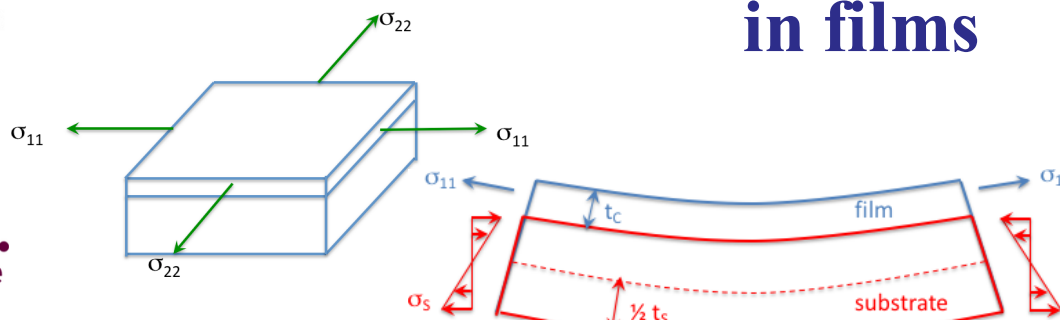


J. Phys Chem C 116 7658-7663 (2012)

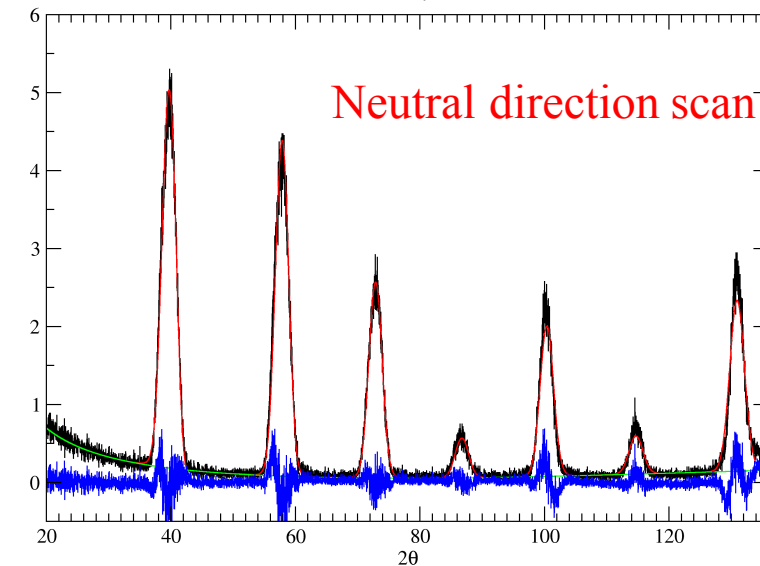
Monitoring the particle contacts in mesoporous ceria as a function of the annealing T



Inhomogeneous strain in films



W: P05 scan $2\theta/\theta$, $\chi=41.32$ $\Delta\omega=0.4345$
 $a=3.1694(3)$ Å (asym, no eccentric)



But the regular ψ -scan method
unfortunately probes a volume that changes
as a function of ψ , averaging out the strain
in the film, and preventing a mapping of
the local strain

Measuring the local strain in glancing geometry

- $\psi = \alpha - \theta(hkl)$

ψ angle should be re-encoded in glancing geometry

$$\tau = \frac{\sin \alpha \sin (2\theta - \alpha)}{\mu [\sin \alpha + \sin (2\theta - \alpha)]}$$

The depth τ probed by X-rays is now a function of the impinging angle

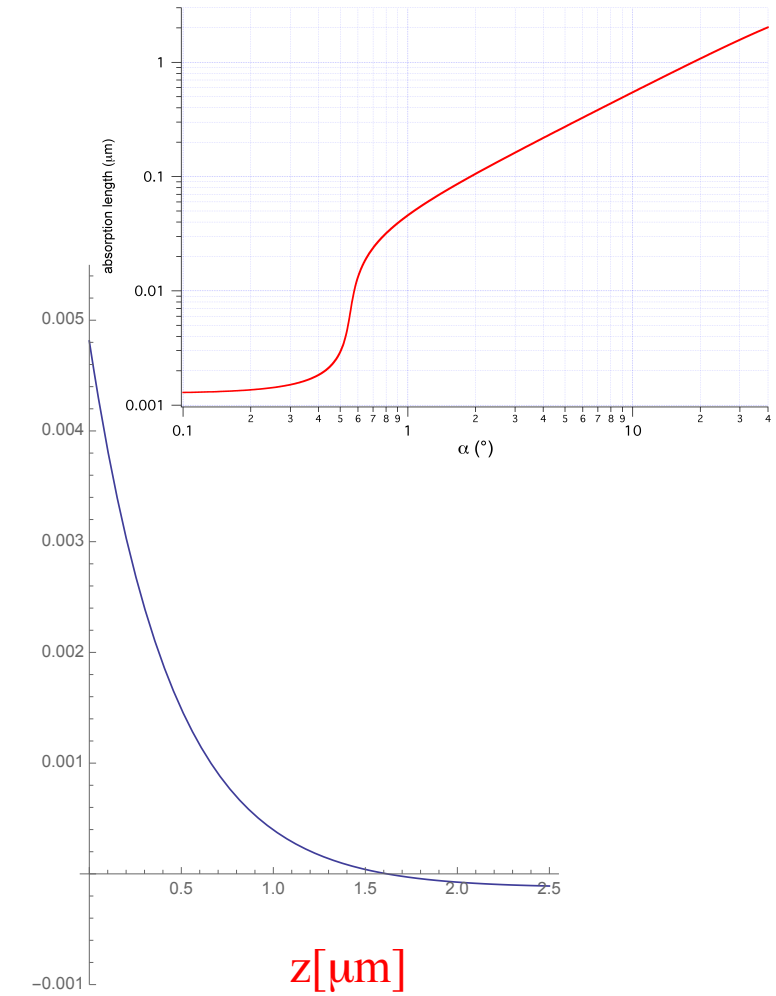
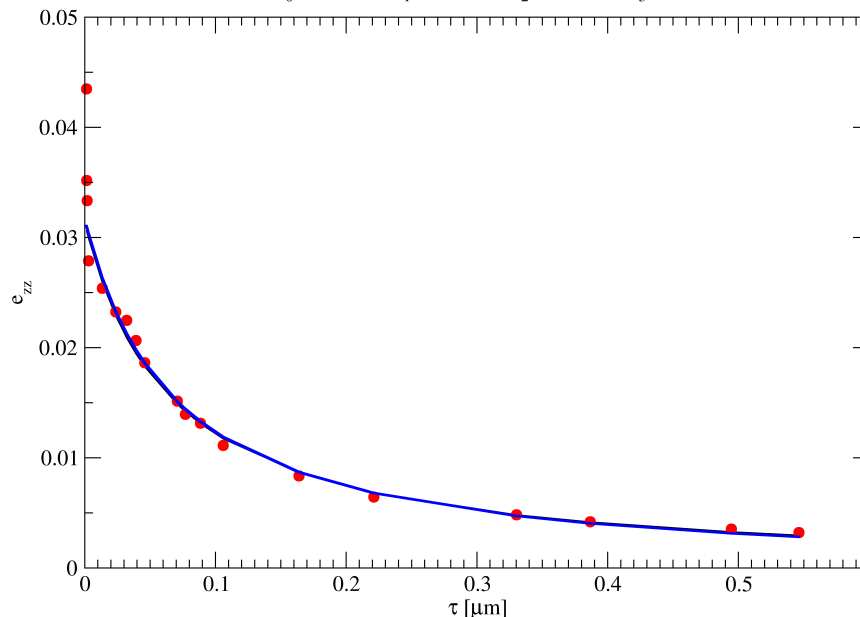
$$\langle \epsilon_{\varphi\psi} \rangle = \frac{\int_0^t \epsilon_{\varphi\psi}(z) \exp\left(-\frac{z}{\tau}\right) dz}{\int_0^t \exp\left(-\frac{z}{\tau}\right) dz}$$

The average strain in a film of thickness t is still averaged by the way we measure (Fredholm's integral)

$$\langle \epsilon_{\varphi\psi} \rangle = \frac{1}{\tau} \int_0^\infty \epsilon_{\varphi\psi}(z) \exp\left(-\frac{z}{\tau}\right) dz = \frac{1}{\tau} \mathcal{L} \left(\epsilon_{\varphi\psi}(z), \frac{1}{\tau} \right)$$

$$\epsilon_{\varphi\psi}(z) = \mathcal{L}^{-1} (\tau \langle \epsilon_{\varphi\psi} \rangle, z)$$

If t is larger than the probed depth τ the Fredholm's integral becomes a Laplace transform that can be inverted, thus providing the value of the local strain at each value z in the film



Conclusion

- GAXRD & materials modelling - global approach to understand complex systems :
 - Elementary mechanisms
 - Chemistry, crystal structure
 - (Meso) Microstructures
- Understand the property changes
- Point out the key issues to design new/better materials for advanced technologies